

Review

Proton transfer to synthetic Fe–S-based clusters

Richard A. Henderson*

Chemistry, School of Natural Sciences, University of Newcastle, Bedson Building, Newcastle upon Tyne NE1 7RU, UK

Received 16 August 2004; accepted 10 December 2004

Available online 6 February 2005

Contents

1. Introduction	1841
2. Protonation of synthetic Fe–S-based clusters	1842
2.1. Protonation with $[\text{NH}_4\text{Et}_3]^+$: single protonation of the cluster core	1842
2.2. Protonation with $[\text{lutH}]^+$: diprotonation of the cluster core	1847
2.3. Rates of proton transfer to Fe–S-based clusters	1848
2.4. Electronic effects on the rates of proton transfer	1852
3. Protonation and the action of nitrogenase	1853
3.1. The binding of substrates by nitrogenases	1853
3.2. Protonation of nitrogenase cofactors and dihydrogen production	1854
4. Summary	1855
References	1856

Abstract

The protonation chemistry of synthetic Fe–S-based clusters containing cuboidal $\{\text{Fe}_4\text{S}_4\}$ or $\{\text{MoFe}_3\text{S}_4\}$ cores is described with an emphasis on: the number of protons that bind to the clusters; where the protons bind; the $\text{p}K_{\text{a}}$'s of the protonated clusters; the rates of proton transfer and how the metal composition of the cluster influences all these factors. The results from the studies on the synthetic Fe–S-based clusters reveal general reactivity patterns, which it is anticipated, would also be operating, in natural Fe–S-based clusters. In particular, we consider the action of the active sites of the nitrogenases, and how the metal composition of the active site may modulate the reactivity of the enzyme. The relative efficiencies of the three principal nitrogenases (Mo-nitrogenase, V-nitrogenase and Fe-only-nitrogenase) have been rationalised by consideration of the binding affinities and protonation reactivities of synthetic clusters. It is proposed that the presence of Mo in cofactor leads to higher binding affinity for dinitrogen and a slower rate of proton transfer, and hence slower rate of dihydrogen production than the V-cofactor or Fe-only-cofactor. It is proposed that Mo in cofactor facilitates nitrogen fixation by suppressing the hydrogenase behaviour of the active site.

© 2005 Elsevier B.V. All rights reserved.

Keywords: Iron–sulfur clusters; Mechanism; Protonation; Nitrogenases

1. Introduction

When you consider Fe–S clusters the immediate thought is of electron transfer reactions [1]. Undoubtedly, this is the most common reaction of natural Fe–S clusters but other bi-

ological roles for Fe–S-based clusters have now emerged. Most notably, in certain enzymes the active site is a Fe–S-based cluster [2]. An enzyme, which has been the focus of our studies for several years, has been nitrogenase. This enzyme converts N_2 into NH_3 by a sequence of coupled electron- and proton-transfer reactions under ambient conditions. The enzyme performs this chemistry at a structurally unique Fe–S-based cluster called cofactor, by a mechanism, which is still

* Tel.: +44 191 222 6636; fax: +44 191 222 6929.

E-mail address: r.a.henderson@ncl.ac.uk.

undefined at the molecular level. Since protons are essential for the conversion of the N_2 into NH_3 , it is evident that the cofactor must operate in a protic environment.

The ability of synthetic Fe–S-based clusters to bind protons is one of their most fundamental and ubiquitous reactions. In this article, I will summarise some of our findings on the protonation chemistry of synthetic Fe–S-based clusters. Whilst the mechanistic chemistry of synthetic Fe–S-based clusters is sufficiently interesting in its own right to warrant investigation, our studies also add to the general understanding of how the active sites of Fe–S-based metalloenzymes operate. At the end of the article, one aspect of the reactivity of nitrogenases will be discussed in the light of the protonation chemistry of synthetic Fe–S-based clusters. This aspect is the limiting stoichiometries of the nitrogenases.

2. Protonation of synthetic Fe–S-based clusters

This article will focus on the reactivities of cuboidal Fe–S-based clusters containing the $\{Fe_4S_4\}$ or $\{MoFe_3S_4\}$ cores, such as $[Fe_4S_4X_4]^{2-}$ and the dicubanes $[\{MoFe_3S_4X_3\}_2(\mu-SR)_3]^{3-}$ ($X = Cl$ or RS ; $R = \text{alkyl}$ or aryl). The Mo sites in the dicubanes are six coordinate and substitutionally inert. Consequently, studies on these clusters allow us to probe how the presence of Mo within a cluster core modulates the reactivity of the remaining Fe and S centres.

2.1. Protonation with $[NH_4Et_3]^+$: single protonation of the cluster core

That synthetic Fe–S clusters can be protonated has been appreciated since the earliest days of this area of chemistry. In 1975, Dukes and Holm reported the first kinetic study on the reactions of synthetic Fe–S clusters. In this study, the authors determined the kinetics for the substitution reactions of the terminal alkyl thiolate in $[Fe_4S_4(SR)_4]^{2-}$ ($R = Bu^t$) with a range of 4-substituted arylthiols [3]. The kinetics of the substitution of the alkyl thiolate ligand by an arylthiol obeys a

simple overall second order rate law: first order dependence on the concentrations of cluster and thiol. Furthermore, the rate of the reaction was faster for the more acidic thiols (i.e., those with the more electron-withdrawing 4-R-substituents). It was proposed, that protonation (from the thiol) to the cluster was involved in the substitution reaction, and it seemed reasonable to suggest that protonation occurred probably to the coordinated thiolate, as shown in Fig. 1. Furthermore, it was proposed that the proton-transfer step was rate limiting.

During the 1990s, we were interested in the protonation reactions of transition metal complexes, and the work of Dukes and Holm awoke our interest in the reactions of Fe–S-based clusters. We decided to study the reactivity of Fe–S-based clusters in a little more detail. Revitalisation of the mechanistic chemistry of synthetic Fe–S-based clusters nearly 20 years after the original studies had a significant advantage. The synthetic chemistry of Fe–S-based clusters had made major advances in the intervening years resulting in a wide range of different Fe–S-based clusters. Consequently, a systematic investigation of the effect of cluster composition, cluster redox state and cluster topology on the reaction mechanisms could be undertaken. The first reaction type we set out to study was the substitution reaction and the effect of acid on the rate of this process. Effectively, we wanted to study the same type of reaction as that shown in Fig. 1, but we did not want to use this system. The major disadvantage of the Dukes and Holm study is that the thiol is playing several roles in this reaction: it is the nucleophile, the acid and (after deprotonation) the conjugate base. We wanted to be able to distinguish these three roles and also be able to independently control the concentrations of the acid, base and nucleophile in the mixture.

The system we developed for studying the substitution reactions of Fe–S-based clusters in the presence of acid is shown in Fig. 2. This figure shows the substitution reaction of the cuboidal $[Fe_4S_4X_4]^{2-}$ cluster. However, it is important to appreciate that the system is entirely general: we can study the reaction of any synthetic Fe–S cluster under comparable conditions. Indeed, it is the comparison of

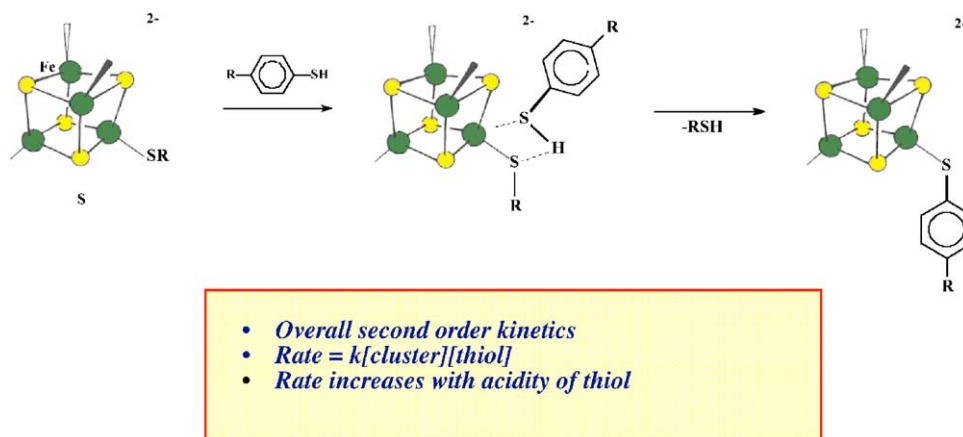


Fig. 1. Summary of the kinetics and mechanism of the reaction between $[Fe_4S_4(Salkyl)_4]^{2-}$ and 4- RC_6H_4SH in MeCN.

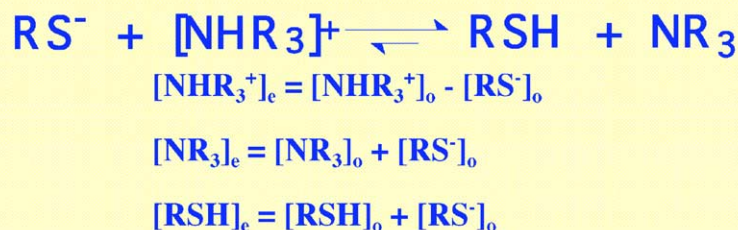
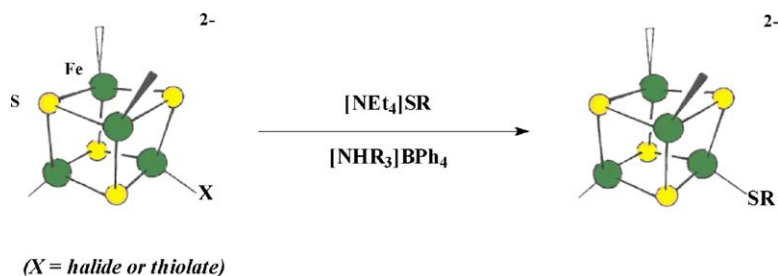


Fig. 2. System used for the study of the kinetics of the reaction between $[\text{Fe}_4\text{S}_4(\text{SR})_4]^{2-}$ and $\text{R}'\text{SH}$ in the presence of $[\text{NHR}_3]^+$ and NR_3 in MeCN.

a variety of different clusters, which allow us to establish general reactivity patterns for the whole family of Fe–S-based clusters [4–6]. The solvent used is acetonitrile. This has several advantages. First, the synthetic Fe–S-based clusters are invariably soluble in that solvent and secondly, there is a lot of quantitative information about the nature of solution species in this solvents. In particular, we know the pK_a 's of acids in this solvent. In the system shown in Fig. 2, the nucleophile is introduced as a thiolate salt (a tetraalkylammonium salt because of solubility in MeCN). The first acid we used in the studies was $[\text{NHEt}_3]^+$ ($\text{pK}_a = 18.46$ in MeCN) [7]. The acid is provided as the $[\text{BPh}_4]^-$ salt since this anion is effectively inert and thus will not be involved in reactions which would complicate the system and the kinetic analysis. Subsequently other ammonium ions have been employed such as the stronger acid $[\text{lutH}]^+$ ($\text{pK}_a = 15.4$ in MeCN lut = 2,6-dimethylpyridine) [8], and the weaker acid $[\text{H}_2\text{N}(\text{CH}_2)_3\text{CH}_2]^+$ ($\text{pK}_a = 21.5$ in MeCN) [9,10]. Ammonium cations are good acids for synthetic Fe–S-based clusters because they are sufficiently strong to be able to protonate the cluster, but not so strong an acid that they decompose the cluster. A crucial requirement is that the clusters retain their integrity throughout the reaction.

In mixtures containing RS^- and $[\text{NHEt}_3]^+$, the equilibrium shown in Fig. 2 is rapidly established. Provided the concentration of acid is greater than the concentration of thiolate then the equilibrium lies completely to the right hand side, and the concentrations of all reactants can be calculated from the relationships shown in Fig. 2. In the presence of an excess of $[\text{NHEt}_3]^+$, it is this cation which is the acid, NEt_3 is the base and RSH is the nucleophile. Consequently,

the concentrations of all these reagents can be controlled independently and the true kinetic dependence on each determined. Note that although, strictly speaking, RSH is also an acid, it is a significantly weaker acid (for PhSH , $\text{pK}_a > 19.3$) [10] than $[\text{NHEt}_3]^+$, and so $[\text{NHEt}_3]^+$ always wins out as the acid.

A typical result from the kinetic study is shown in Fig. 3 for the reaction of $[\text{Fe}_4\text{S}_4(\text{SEt})_4]^{2-}$ with PhSH in the presence of mixtures of $[\text{NHEt}_3]^+$ and NEt_3 [4]. The rate of the reaction exhibits a first order dependence on the concentration of cluster but is completely independent of the concentration of nucleophile (PhSH). However, the reaction exhibits a non-linear dependence on the ratio $[\text{NHEt}_3^+]/[\text{NEt}_3]$ as shown in Fig. 3. Before moving on to discuss the mechanism associated with these kinetics, there are two important points which need to be emphasised. First, the rate depends only on the ratio $[\text{NHEt}_3^+]/[\text{NEt}_3]$, and not on the absolute concentrations of either reagent. Secondly, that the rate depends only on $[\text{NHEt}_3^+]/[\text{NEt}_3]$ (and not, for example, $[\text{NHEt}_3^+]^2/[\text{NEt}_3]^2$) indicates only one proton binds to the cluster with this acid. The reader may consider this to be an unnecessary point to make, but the importance of this statement will become clear in the subsequent discussion.

Inspection of the curve in Fig. 3 shows that when $[\text{NHEt}_3^+] = 0$, the reaction occurs at a finite rate. This corresponds to the uncatalysed substitution reaction, which can be studied independently, in the absence of acid. As the concentration of acid increases the rate increases, such that at low values of $[\text{NHEt}_3^+]/[\text{NEt}_3]$, the reaction exhibits a first order dependence on $[\text{NHEt}_3^+]/[\text{NEt}_3]$, but at high values of $[\text{NHEt}_3^+]/[\text{NEt}_3]$, the rate of the reaction becomes independent of this ratio. The rate law derived from these data

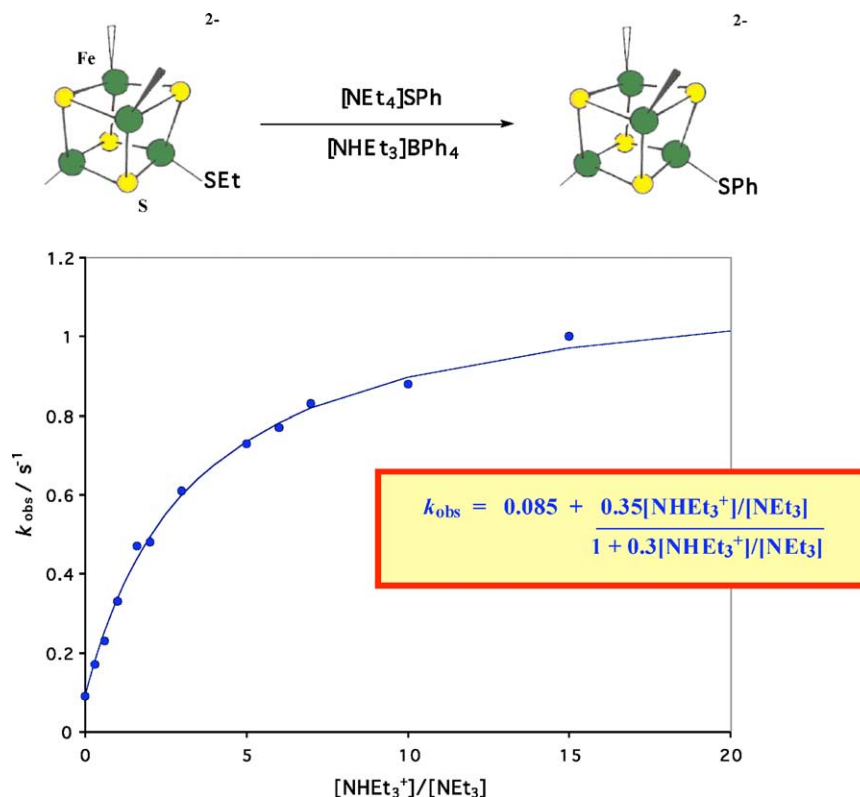


Fig. 3. Kinetics for the substitution reaction of $[\text{Fe}_4\text{S}_4(\text{SEt})_4]^{2-}$ with PhSH in the presence of $[\text{NHEt}_3]^+$ and NEt_3 in MeCN . The rate exhibits a first order dependence on the concentration of cluster and is independent of the concentration of the nucleophile. The dependence of k_{obs} on $[\text{NHEt}_3^+]/[\text{NEt}_3]$ is shown in the box.

is described by the equation shown in Fig. 3. This rate law is consistent with an acid-catalysed dissociative substitution mechanism as shown in Fig. 4.

At the top of Fig. 4 is shown the uncatalysed pathway, which operates in the absence of acid. In this article, I will not discuss the uncatalysed pathway. Suffice it to say that for $[\text{Fe}_4\text{S}_4(\text{SEt})_4]^{2-}$, the mechanism is dissociative and involves rate-limiting dissociation of an ethanethiolate ligand to generate a cluster where one of the Fe atoms has a vacant site.

The vacant site can be attacked by the excess of the nucleophile (PhS^-) present in the solution and complete the first act of substitution.

In the presence of acid, protonation of the cluster can occur at a rate, which is faster than that of the dissociation of the ethanethiolate in the uncatalysed pathway. This protonation occurs somewhere on the cluster (we will discuss where later) and labilises the cluster to dissociation of an ethanethiolate ligand. The vacant site thus created on one of the Fe sites is

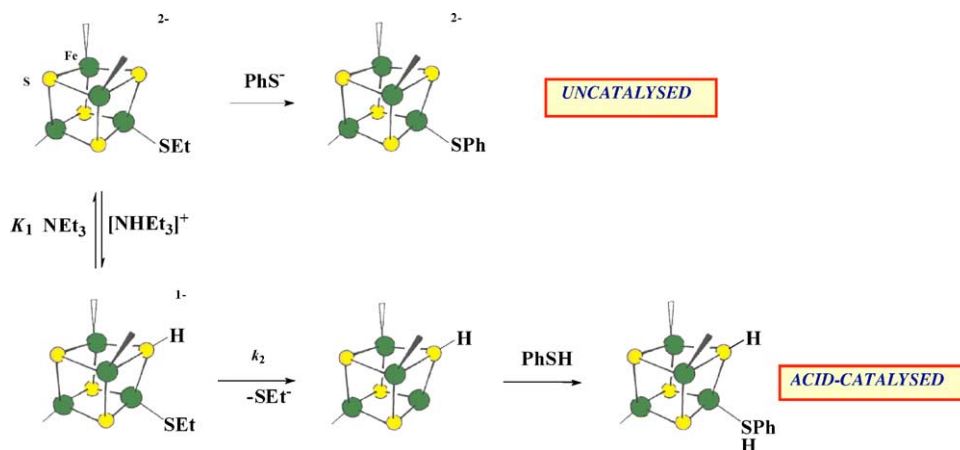


Fig. 4. Mechanism for the substitution reaction of $[\text{Fe}_4\text{S}_4(\text{SEt})_4]^{2-}$ with PhSH in the presence of $[\text{NHEt}_3]^+$ and NEt_3 in MeCN . The top line gives an indication of the uncatalysed pathway.

now attacked by the nucleophile (which in the presence of an excess of acid is PhSH). The pathway shown in Fig. 4 is entirely general for *all* Fe–S-based clusters with one provision. For some clusters, the act of substitution (the k_2 step) can be associative and hence exhibits a dependence on the concentration of nucleophile [11].

Comparison of the rate of dissociation of the leaving group from $[\text{Fe}_4\text{S}_4(\text{SEt})_4]^{2-}$ (intercept of plot in Fig. 3) and the protonated cluster (limiting rate constant at high $[\text{NH}_4\text{Et}_3^+]/[\text{NEt}_3]$) shows that protonation of the cluster facilitates dissociation of the leaving group. This is an entirely general feature observed with all singly protonated Fe–S-based clusters, and we will return to the electronic origins of this behaviour later.

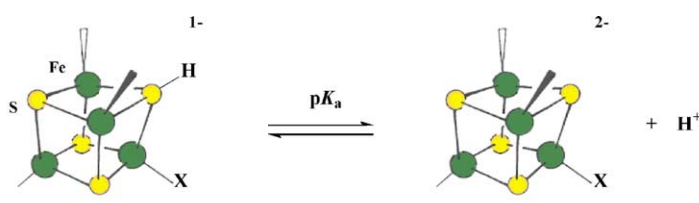
The non-linear dependence on $[\text{NH}_4\text{Et}_3^+]/[\text{NEt}_3]$ observed for these reactions means that we can determine the rate constant for substitution of the protonated cluster (k_2) and the protonation equilibrium constant (K_1). Furthermore, because the solvent is MeCN, and we know that the $\text{p}K_a$ of $[\text{NH}_4\text{Et}_3]^+$ in MeCN is 18.4, we can calculate the $\text{p}K_a$ of the protonated cluster. The results from studies on a wide range of different Fe–S-based clusters are summarised in Fig. 5 [4–6,12–15].

The results for the clusters presented in Fig. 5 have been divided into two sections: for those clusters containing terminal chloro-ligands (top) and for those clusters containing terminal thiolate ligands (bottom). Closer inspection shows that in the latter section the clusters contain either alkyl or aryl thiolate ligands. In addition, looking at all the clusters we see that there is a variety of overall charges on the clusters; that some clusters are cuboidal $\{\text{Fe}_4\text{S}_4\}$ clusters whilst others contain a Mo and are based on the $\{\text{MoFe}_3\text{S}_4\}$ core.

Finally, there is a range of different nuclearities in the clusters presented in Fig. 5: binuclear, trinuclear, tetranuclear and hexanuclear. Despite all these variations, it is very noticeable that for *all* synthetic Fe–S-based clusters, the $\text{p}K_a$ falls in the range $\text{p}K_a = 17.9$ –18.9. The remarkable insensitivity of the $\text{p}K_a$ in this wide variety of Fe–S-based clusters indicates that protonation is not occurring at a terminal ligand, but rather is occurring at a site which is common to all the clusters. It seems most likely that the protonation site in all the clusters is the bridging sulfur atom.

Consistent with our proposal that protonation of bridging sulfur sites is the major labilising force in the substitution reactions involving acid, the reactions of $[\text{M}_4(\text{SPh})_{10}]^{2-}$ ($\text{M} = \text{Fe}$ or Co) [16] with either PhSH or $[\text{M}'\text{S}_4]^{2-}$ ($\text{M}' = \text{Mo}$ or W) are unperturbed by the presence of $[\text{NH}_4\text{Et}_3]^+$. Interestingly, substitution of the terminal PCy_3 ligands in $[\text{Fe}_4\text{S}_4(\text{PCy}_3)_4]$ by PhSH, in the presence of $[\text{NH}_4\text{Et}_3]^+$, is acid independent. Although $[\text{Fe}_4\text{S}_4(\text{PCy}_3)_4]$ contains $\mu_3\text{-S}$ sites, the phosphines are sufficiently bulky to stop the sterically-demanding $[\text{NH}_4\text{Et}_3]^+$ approaching the sulfur sites to be protonated [12].

The kinetics of the substitution of terminal ligands on Fe–S-based clusters [12] such as $[\text{Fe}_2\text{S}_2\text{Cl}_4]^{2-}$, $[\text{Fe}_4\text{S}_4\text{X}_4]^{2-}$, $[(\text{MoFe}_3\text{S}_4\text{X}_3)_2\{\mu\text{-SEt}\}_3]^{3-}$, $[(\text{MoFe}_3\text{S}_4\text{X}_3)_2\{\mu\text{-Fe}(\text{SEt})_6\}]^{3-}$ ($\text{X} = \text{alkyl thiolate, aryl thiolate or halide}$), $[\text{S}_2\text{MS}_2\text{FeCl}_2]^{2-}$ ($\text{M} = \text{Mo}$ or W), $[\text{Cl}_2\text{FeS}_2\text{VS}_2\text{FeCl}_2]^{3-}$ and $[\text{MoFe}_4\text{S}_6(\text{PET}_3)_4\text{Cl}]$ are all catalysed by $[\text{NH}_4\text{Et}_3]^+$. Whilst, it is not unreasonable that bridging sulfur atoms are the most basic sites in clusters containing terminal chloro-ligands, there must be some concern that in clusters containing terminal thiolate ligands, the thiolate sulfur is more basic



	Cluster	$\text{p}K_a$
<i>Fe-Cl clusters:</i>	$[\text{Cl}_2\text{FeS}_2\text{VS}_2\text{FeCl}_2]^{3-}$	17.9
	$[\text{S}_2\text{MoS}_2\text{FeCl}_2]^{2-}$	17.9
	$[\text{Fe}_4\text{S}_4\text{Cl}_4]^{2-}$	18.8
	$[(\text{MoFe}_3\text{S}_4\text{Cl}_3)_2(\mu\text{-SEt})_3]^{3-}$	18.6
	$[\text{Fe}_2\text{S}_2\text{Cl}_3(\text{NCMe})]^-$	18.1
	$[\text{Fe}_6\text{S}_6\text{Cl}_2(\text{PET}_3)_4]$	18.0
<i>Fe-SR clusters:</i>	$[\text{Fe}_4\text{S}_4(\text{SPh})_4]^{2-}$	18.6
	$[\text{Fe}_4\text{S}_4(\text{SEt})_4]^{2-}$	18.0
	$[(\text{MoFe}_3\text{S}_4(\text{SEt})_3)_2(\mu\text{-SEt})_3]^{3-}$	18.1

Fig. 5. Summary of the $\text{p}K_a$ of the protonated Fe–S-based clusters in MeCN at 25.0 °C.

than any bridging sulfur site. However, if thiolate ligands are being protonated in (for example) $[\text{Fe}_4\text{S}_4(\text{SEt})_4]^{2-}$, our kinetic studies are not detecting this protonation. This discussion highlights a limitation to the method we have used to study protonation reactions. It is worth emphasising this limitation at this stage.

The simplest and most direct method to look at the protonation of any cluster is to monitor the reaction of the cluster with acid. Unfortunately, the addition of a proton to Fe–S-based clusters is effectively spectroscopically silent. The electronic spectrum of Fe–S-based clusters is dominated by intense bands associated with electronic transitions of the cluster core, and addition of a proton to the cluster has negligible effect on the spectrum. The I.R. spectral bands associated with S–H bonds are notoriously difficult to detect because they are weak and broad. The ^1H NMR spectra of Fe–S-based clusters are paramagnetically shifted and we have been unable to detect the peak due to the single S–H group. The problem of detecting the broad resonance of a single proton whose position will be paramagnetically shifted is compounded by the likelihood that this proton is rapidly exchanging and hence the peak will be further broadened.

Because of these problems, we have used the kinetic method described in this section to detect the protonation of the cluster. Effectively, we have coupled proton transfer to

a substitution reaction. The substitution reaction is associated with significant changes in the UV–vis absorption spectrum. Thus, if a proton binds and affects the lability of the cluster we will be able to detect the protonation. However, if protons bind to a site on the cluster, which does not appreciably affect the lability of the cluster, we will not detect this protonation. Thus, in $[\text{Fe}_4\text{S}_4(\text{SEt})_4]^{2-}$, if protonation at a thiolate does occur (and this seems likely), it does not affect the rate of substitution, indicating that protonation of the cluster core ($\mu_3\text{-S}$) is more labilising than protonation of terminal thiolate ligands.

A likely mechanism for the reaction of $[\text{Fe}_4\text{S}_4(\text{SEt})_4]^{2-}$ with PhSH in the presence of $[\text{NHEt}_3]^+$ is shown in Fig. 6. This mechanism is an elaboration of that shown in Fig. 4. Initial protonation occurs at the basic thiolate sulfur but protonation at this site has no detectable effect on the rate of substitution of the cluster. It is only upon protonation of the bridged sulfur site that the lability of the cluster is significantly affected.

That protonation of the coordinated thiolate is not labilising, but further protonation of the bridging sulfur site is, can be rationalised by the bonding description shown in Fig. 7. Protonation of the coordinated thiolate produces the corresponding thiol in which the S-to-Fe σ -bond is weakened but the Fe-to-S π -backbonding is increased. The overall effect is

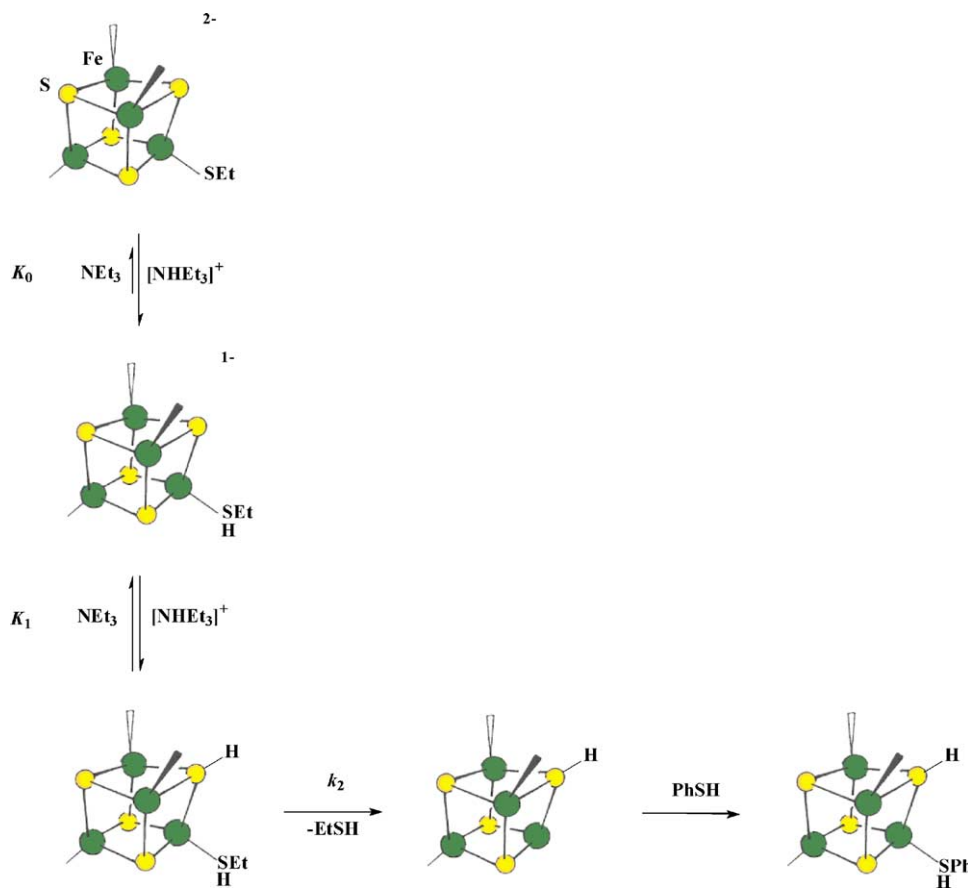


Fig. 6. Mechanism for the substitution reaction of $[\text{Fe}_4\text{S}_4(\text{SEt})_4]^{2-}$ with PhSH in the presence of $[\text{NHEt}_3]^+$ and NEt_3 in MeCN, showing protonation of the $\mu_3\text{-S}$ (detected in the kinetics) and protonation of the thiolate (undetected but presumed).

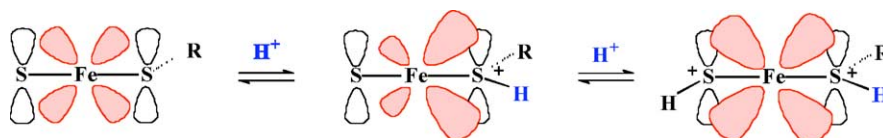


Fig. 7. Representation of the bonding between Fe, thiolate and bridging sulfur in Fe-S-based clusters, and the effect of protonation at thiolate and then bridging sulfur.

that the bond strengths of Fe-thiolate and Fe-thiol are similar and hence there is little change in lability. The same sort of effect has been observed reflected in the bond lengths of mononuclear Fe-thiolate and Fe-thioether complexes [17]. In the Fe-S clusters, the protonation of a bridging sulfur site appears to have the effect of competing for the π -backbonding to the thiol and thus labilising the thiol to dissociate.

2.2. Protonation with $[lutH]^+$: diprotonation of the cluster core

The studies with $[NHEt_3]^+$ indicate that protonation of the cluster core catalyse the substitution of either terminal thiolate or terminal chloro-ligands. Use of the stronger acid $[lutH]^+$ ($pK_a = 15.4$ in MeCN) results in diprotonation of the cluster core and the substitution reactions of the clusters are perturbed in an unexpected manner by the addition of this second proton [12,18]. It is important to note that, because the first protonation of the cluster core is associated with $pK_a = 17.9$ – 18.9 , even at the lowest concentration of $[lutH]^+$ used the clusters are singly protonated. Consequently, the kinetics of the substitution reactions of synthetic Fe-S-based in the presence of $[lutH]^+$ reflects only the addition of the second proton to the cluster core.

For clusters with terminal thiolate ligands, such as $[Fe_4S_4(SET)_4]^{2-}$, addition of the second proton to the cluster core leads to further labilisation of the cluster. The rate of the reaction exhibits a non-linear dependence on the ratio $[lutH^+]/[lut]$. At low values of $[lutH^+]/[lut]$, the rate varies linearly with the ratio but, at high values of $[lutH^+]/[lut]$, the rate becomes independent of the ratio and dissociation of the coordinated thiolate becomes rate limiting. Under these conditions, all the clusters have two protons bound to the core. The successive addition of two protons to the core of $[Fe_4S_4(SET)_4]^{2-}$ results in a regular increase in the lability of the thiolate.

Studies on the kinetics of the acid-catalysed substitution reactions of $[Fe_4S_4Cl_4]^{2-}$ in the presence of $[lutH]^+$ shows a quite distinctly different behaviour [18]. Even at the lowest concentration of $[lutH]^+$, $[Fe_4S_4Cl_4]^{2-}$ is singly protonated, presumably at the core since the chloro-groups are insufficiently basic to be protonated by $[lutH]^+$. However, increasing the concentration of $[lutH]^+$ results in a decrease in the rate. Thus, whilst addition of the first proton to the cluster catalyses the associative substitution reaction, addition of the second proton results in inhibition of the associative substitution reaction. The sequence of protonation steps is shown in Fig. 8.

The bonding picture shown in Fig. 7 indicates how protonation of a single μ_3 -S in a Fe-S-based cluster labilises a terminal thiol by competing for the π -backbonding to the terminal thiol. Extension of this model would rationalise why protonation of two μ_3 -S in a Fe-S-based cluster would lead to further labilisation of the dissociation of the thiol. Such a simple consideration is adequate for $[Fe_4S_4(SR)_4]^{2-}$ where the substitution is dissociative. However, for associative substitution mechanisms, as observed in $[Fe_4S_4Cl_4]^{2-}$, more detailed reflection is needed.

In the associative pathway, there are two distinguishable steps: the binding of the nucleophile and the dissociation of the leaving group. Protonation of a μ_3 -S would reasonably be expected to favour attack of the nucleophile to the adjacent Fe site but suppress dissociation of the incipient anionic chloro-group. It would appear that single protonation most influences the binding of the nucleophile, but the second protonation leads to a marked decrease in the rate of dissociation of the chloro-leaving group.

In the same way, as we determined the pK_a for the first protonation of the cluster core in studies with $[NHEt_3]^+$, we can, in studies with $[lutH]^+$, calculate pK'_a for addition of the second proton to the cluster core. Interestingly, pK'_a for the second protonation of the cluster core shows a marked dependence on the nature of the terminal ligand. Whilst the pK_a of all Fe-S-based clusters singly protonated on the cluster core is essentially invariant, the pK'_a associated with the second protonation of the cluster core depends on the terminal ligands (ca. 16.5 for chloro-clusters and ca. 13.5 for thiolato-clusters). This is probably a consequence of the electronic response of the terminal ligand to the addition of the first protonation.

Addition of the first proton to $[Fe_4S_4X_4]^{2-}$ ($X = RS$ or Cl) produces $[Fe_4S_3(SH)X_4]^-$. This protonation must have an effect on all the Fe-S and Fe-X bond lengths in the cluster. The insensitivity of the protonation constant to the identity of the cluster (and most particularly the terminal ligands) is consistent with the changes to the bond lengths associated with the chloro- and thiolate ligands responding similarly to the addition of the first proton. Furthermore, the electron density at the sulfur sites would be expected to be modulated by the bonding in Fe-X and the similarities of the pK_a 's of $[Fe_4S_4X_4]^{2-}$ indicate the electronic influence of thiolate and chloro-ligands is similar.

The binding of the second proton is also assumed to occur at a sulfur atom. However, the binding constant for the second proton is significantly different depending on whether the cluster contains chloro- or thiolate ligands. It appears

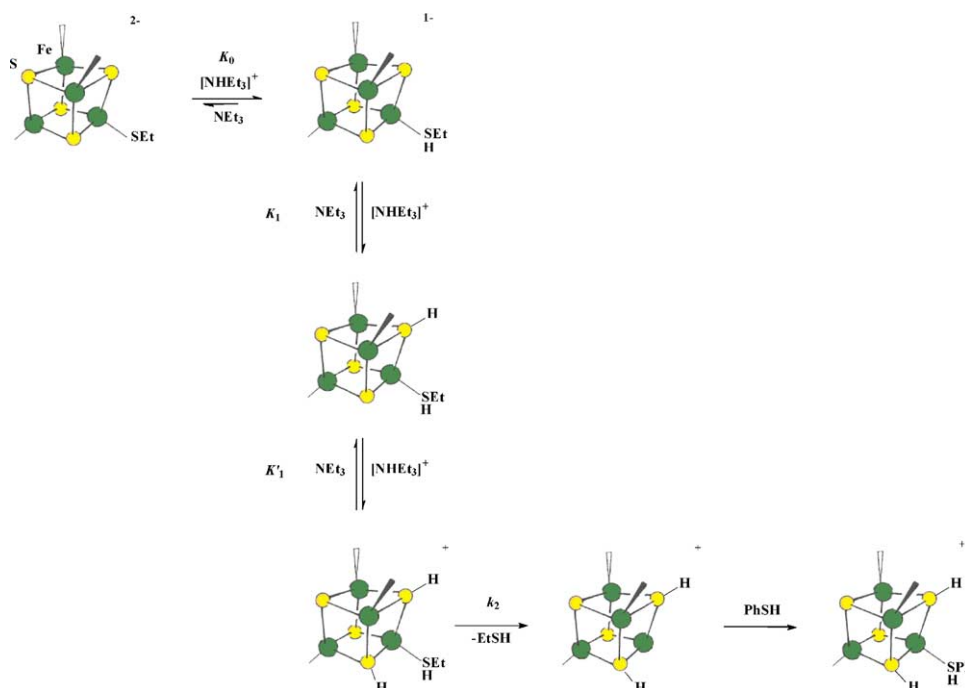


Fig. 8. Mechanism for the substitution reaction of $[\text{Fe}_4\text{S}_4(\text{SET})_4]^{2-}$ with PhSH in the presence of $[\text{lutH}]^+$ and lut in MeCN, showing the undetected but presumed protonation of the thiolate and the detected protonation of two $\mu_3\text{-S}$ sites.

that the bonding of the chloro-ligands effectively neutralizes the positive charge introduced with the first protonation so that addition of the proton to $[\text{Fe}_4\text{S}_3(\text{SH})\text{Cl}_4]^-$ is associated with a $\text{p}K'_a$ which is only 2 units from $\text{p}K_a$. In contrast with $[\text{Fe}_4\text{S}_3(\text{SH})(\text{SR})_4]^-$, it appears that the thiolate-ligands do not so effectively neutralize the positive charge. Consequently, the binding of the second proton is associated with a $\text{p}K'_a$, which is 4–5 units different to the $\text{p}K_a$. The chloro-ligands are better than thiolate ligands at compensating for the increased positive charge on the cluster.

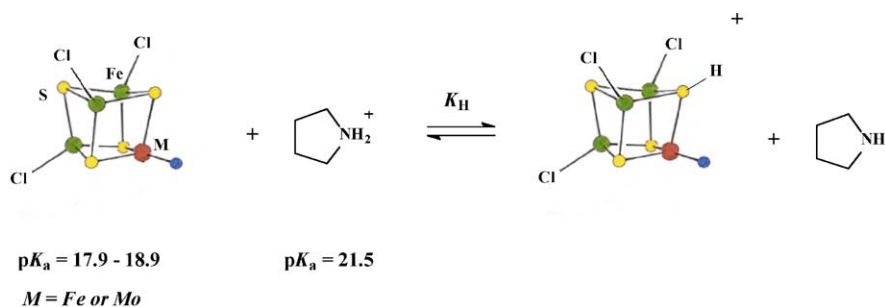
2.3. Rates of proton transfer to Fe–S-based clusters

In all the studies described above, the mechanism is accurately described as an acid-catalysed substitution reaction. In other words, the protonation step is an initial equilibrium reaction which is rapidly established prior to the act of substitution. Consequently, although much information can be obtained from these studies (such as the $\text{p}K_a$'s of the clusters, the effect that protonation has on the act of substitution and the mechanism of substitution), we get very little information about how rapidly proton transfer occurs to the cluster core. We can establish lower limits for the protonation of $[\text{Fe}_4\text{S}_4\text{Cl}_4]^{2-}$ with $k \geq 2 \times 10^5 \text{ dm}^3 \text{ mol}^{-1} \text{ s}^{-1}$, but this still leaves a large range between 10^5 and the diffusion-controlled limit ($10^{10} \text{ dm}^3 \text{ mol}^{-1} \text{ s}^{-1}$).

One of the main reasons why proton transfer to Fe–S-based clusters from $[\text{NHEt}_3]^+$ or $[\text{lutH}]^+$ is rapid is because the proton transfer is thermodynamically favourable. In order to make proton transfer slow, we have made use of the char-

acteristic feature that all Fe–S-based clusters are associated with $\text{p}K_a = 18.4 \pm 0.5$. As shown in Fig. 9, if we use a very weak acid, such as pyrrolidinium ion $[\text{H}_2\text{N}(\text{CH}_2)_3\text{CH}_2]^+$, $\text{p}K_a = 21.5$ in MeCN) to protonate Fe–S-based clusters then the proton transfer is thermodynamically unfavourable. Under these conditions, the rate constant for proton transfer will be slower than the maximum possible rate and can become rate limiting. We have studied the substitution reactions of $[\text{Fe}_4\text{S}_4\text{Cl}_4]^{2-}$, $[\{\text{MoFe}_3\text{S}_4\text{Cl}_3\}_2(\mu\text{-SET})_3]^{3-}$ and $[\{\text{MoFe}_3\text{S}_4\text{Cl}_3\}_2(\mu\text{-SPh})_3]^{3-}$ with PhS^- in the presence of $[\text{H}_2\text{N}(\text{CH}_2)_3\text{CH}_2]^+$. Because these clusters have terminal chloro-ligands the dominant pathway for substitution is associative. This introduces a slight complication to our kinetics. Because we are now working with an acid where proton transfer is slow, it could be that proton transfer is slower than the binding of the nucleophile to the cluster. We have to consider two possible pathways. In the first pathway, attack of the nucleophile is faster than proton transfer. In the second pathway, the nucleophile is so poor that the cluster is forced to wait for proton transfer to occur from the pyrrolidinium ion. Both of these pathways have been observed: the former when the nucleophile is PhS^- and the latter when the nucleophile is Br^- .

Kinetic studies [10] on the reaction between $[\text{Fe}_4\text{S}_4\text{Cl}_4]^{2-}$ and PhS^- in the presence of $[\text{H}_2\text{N}(\text{CH}_2)_3\text{CH}_2]^+$ shows kinetics with a first order dependence on the concentration of cluster and PhS^- but a complicated dependence on the concentration of $[\text{H}_2\text{N}(\text{CH}_2)_3\text{CH}_2]^+$ as shown in Fig. 10. Thus, at low concentrations of acid, the rate increases with the con-



- Protonation thermodynamically unfavourable ($K_H = 10^{-3} - 10^{-4}$).
- Rate of proton transfer becomes slow.
- Mechanism depends on the strength of the nucleophile.

Fig. 9. Outline of the system used to measure the rates of proton transfer to Fe–S-based cluster. The generic structure shown represents the clusters $[Fe_4S_4Cl_4]^{2-}$, $[MoFe_3S_4Cl_3]_2(\mu-S\text{Et})_3]^{3-}$ or $[MoFe_3S_4Cl_3]_2(\mu-SPh)_3]^{3-}$.

centration of $[H_2N(CH_2)_3CH_2]^+$. However, at high concentration of acid, the rate becomes independent of the concentration of $[H_2N(CH_2)_3CH_2]^+$. This behaviour is reminiscent of that observed with the stronger acids (Figs. 3 and 8). The important difference is that with $[H_2N(CH_2)_3CH_2]^+$ the rate

depends only on the concentration of acid and not on the ratio, $[acid]/[base]$.

There is a further difference between the studies with $[H_2N(CH_2)_3CH_2]^+$ and those with $[NH_4Et_3]^+$ or $[lutH]^+$. With $[NH_4Et_3]^+$ or $[lutH]^+$, the acids are sufficiently strong to protonate any free thiolate, and in the presence of

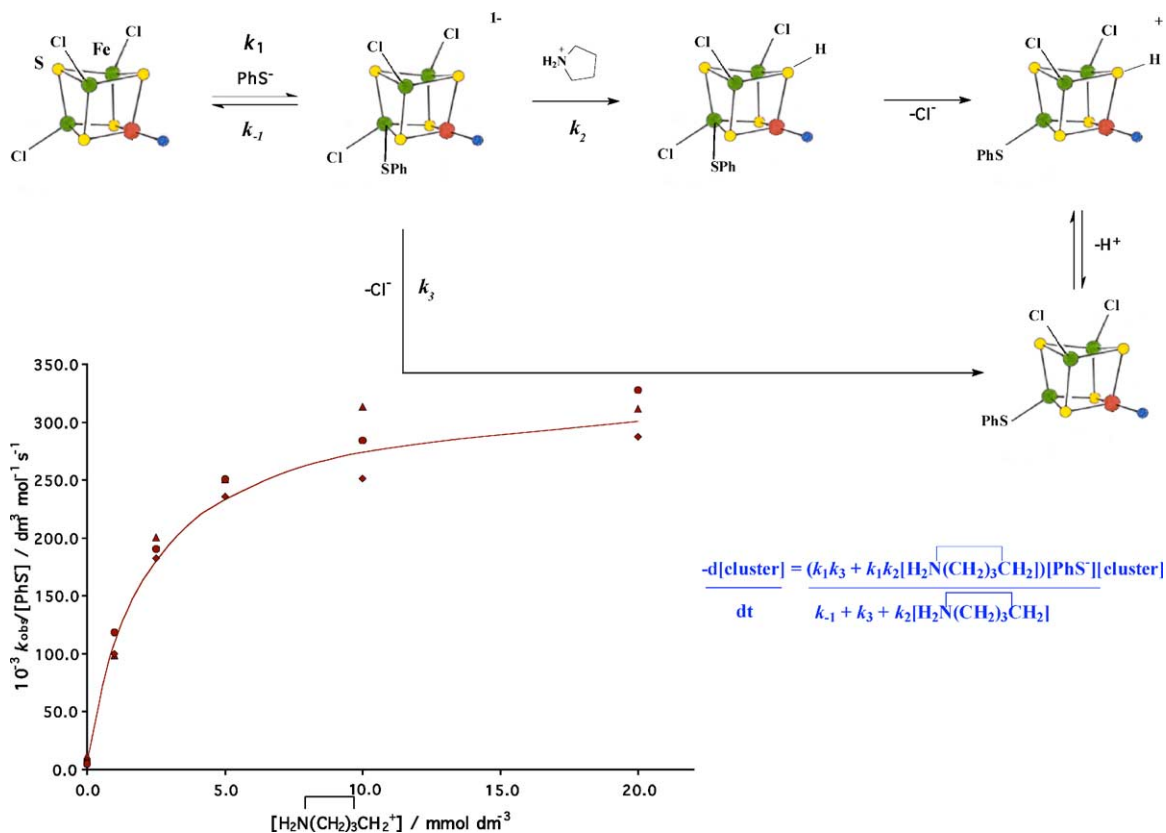


Fig. 10. Kinetics and mechanism for the reaction between Fe–S-based clusters and $[H_2N(CH_2)_3CH_2]^+$ in the presence of PhS^- (strong nucleophile). The clusters studied are $[Fe_4S_4Cl_4]^{2-}$, $[MoFe_3S_4Cl_3]_2(\mu-S\text{Et})_3]^{3-}$ and $[MoFe_3S_4Cl_3]_2(\mu-SPh)_3]^{3-}$.

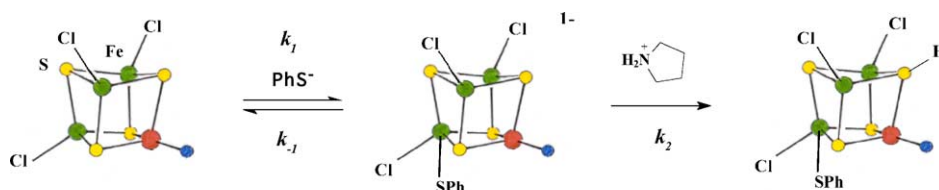
an excess of acid only thiol is present. However, with $[\text{H}_2\text{N}(\text{CH}_2)_3\text{CH}_2]^+$ the acid is insufficiently strong to protonate PhS^- . Consequently, in the reaction of $[\text{Fe}_4\text{S}_4\text{Cl}_4]^{2-}$ with PhS^- in the presence of $[\text{H}_2\text{N}(\text{CH}_2)_3\text{CH}_2]^+$, the nucleophile is PhS^- .

The mechanism of the reaction is shown in Fig. 10. Since $[\text{H}_2\text{N}(\text{CH}_2)_3\text{CH}_2]^+$ protonates the cluster slowly, PhS^- binds to the cluster prior to protonation. The intermediate thus formed is clearly on the pathway to substitution by an acid-independent route. In separate studies, the kinetics of the acid-independent substitution pathway has been determined. As the concentration of acid is increased the rate of protonation of the cluster becomes faster than dissociation of the chloro-ligand and hence more of the reaction proceeds via the pathway involving protonation after binding of the nucleophile.

The rate law associated with the entire mechanism is shown in Fig. 10. It is evident that this is a complicated rate law containing four elementary rate constants. The rate constant we are most interested in calculating is that for the proton transfer (k_2). However, it is clear that this constant cannot be determined from analysis of this complex rate law. However, by just doing one other experiment the value of k_2 can be calculated. Studies in the absence of acid give the kinetics for the acid-independent pathway alone. At high concentrations of PhS^- the observed rate constant is k_3 and hence we can calculate the ratio k_1/k_{-1} . Now, from the studies in the presence of acid, the observed rate constant at high concentrations of $[\text{H}_2\text{N}(\text{CH}_2)_3\text{CH}_2]^+$ corresponds to k_1 . Consequently, we can calculate k_{-1} . Since we now know the values of k_1 , k_{-1} and k_3 , we can calculate the value of k_2

using the expression in Fig. 10. The values of these elementary rates constant for $[\text{Fe}_4\text{S}_4\text{Cl}_4]^{2-}$, $[\{\text{MoFe}_3\text{S}_4\text{Cl}_3\}_2(\mu\text{-SEt})_3]^{3-}$ and $[\{\text{MoFe}_3\text{S}_4\text{Cl}_3\}_2(\mu\text{-SPh})_3]^{3-}$ are summarised in Fig. 11. The rate constants for the proton-transfer reactions are shown in the far right hand column. The notable feature about these rate constants is that they are all about $10^6 \text{ dm}^3 \text{ mol}^{-1} \text{ s}^{-1}$. Consideration of the reaction pathway reveals that although this is a rate constant for proton transfer to the cluster, it is not really the rate constant we want to calculate. The value of k_2 corresponds to the proton transfer from $[\text{H}_2\text{N}(\text{CH}_2)_3\text{CH}_2]^+$ to the cluster containing a bound PhS^- . What we really want to measure is the rate constant for proton transfer from $[\text{H}_2\text{N}(\text{CH}_2)_3\text{CH}_2]^+$ to the parent cluster. It seems reasonable that the binding of the thiolate to the cluster makes the cluster sufficiently basic to be protonated (albeit slowly) by the weak acid and that the rate of proton transfer in these systems is dominated by the presence of the bound thiolate.

The rate constants for proton transfer to Fe–S-based clusters can be measured directly by ensuring that nucleophiles do not bind to the cluster prior to proton transfer. This can be accomplished by using Br^- as the nucleophile. The kinetics and the mechanism of the reaction of Fe–S-based clusters with Br^- in the presence of $[\text{H}_2\text{N}(\text{CH}_2)_3\text{CH}_2]^+$ are shown in Fig. 12. In this system it is evident that the kinetics are much simpler. The rate depends only on the concentrations of cluster and acid, and is independent of the concentration of Br^- . Thus, the gradient of the graphs shown in Fig. 12 correspond to the rate constant for proton transfer from $[\text{H}_2\text{N}(\text{CH}_2)_3\text{CH}_2]^+$ to the cluster.



	$k_1 / \text{M}^{-1} \text{s}^{-1}$	k_{-1} / s^{-1}	$k_2 / \text{M}^{-1} \text{s}^{-1}$
$[\text{Fe}_4\text{S}_4\text{Cl}_4]^{2-}$	1.4×10^5	2.2×10^3	1.8×10^6
$[\{\text{MoFe}_3\text{S}_4\text{Cl}_3\}_2(\mu\text{-SEt})_3]^{3-}$	3.3×10^5	1.3×10^3	6.0×10^6
$[\{\text{MoFe}_3\text{S}_4\text{Cl}_3\}_2(\mu\text{-SPh})_3]^{3-}$	3.8×10^5	1.3×10^3	1.6×10^6

Fig. 11. Summary of the elementary rate constants for the reaction between Fe–S-based clusters and $[\text{H}_2\text{N}(\text{CH}_2)_3\text{CH}_2]^+$ in the presence of PhS^- (strong nucleophile) in MeCN.

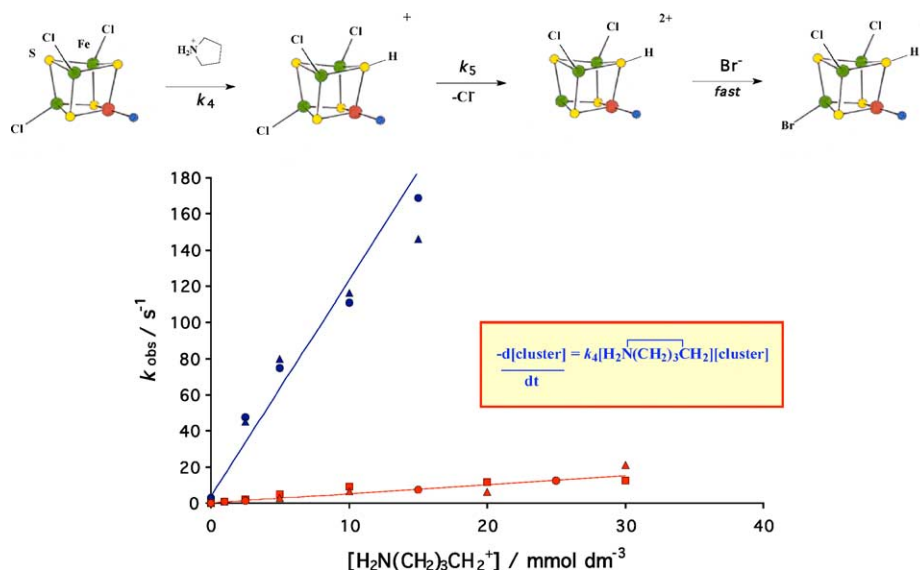


Fig. 12. Kinetics and mechanism for the reaction between Fe-S-based clusters and $[\text{H}_2\text{N}(\text{CH}_2)_3\text{CH}_2]^+$ in the presence of Br^- (weak nucleophile). The clusters studied are $[\text{Fe}_4\text{S}_4\text{Cl}_4]^{2-}$, $[\{\text{MoFe}_3\text{S}_4\text{Cl}_3\}_2(\mu\text{-SEt})_3]^{3-}$ and $[\{\text{MoFe}_3\text{S}_4\text{Cl}_3\}_2(\mu\text{-SPh})_3]^{3-}$.

It is immediately obvious from the graph that $[\text{Fe}_4\text{S}_4\text{Cl}_4]^{2-}$ protonates appreciably faster than either $[\{\text{MoFe}_3\text{S}_4\text{Cl}_3\}_2(\mu\text{-SEt})_3]^{3-}$ or $[\{\text{MoFe}_3\text{S}_4\text{Cl}_3\}_2(\mu\text{-SPh})_3]^{3-}$ [19]. The values of the rate constants and other pertinent data for these reactions are summarised in Fig. 13. There are three important points about these results. (i) The thermodynamic driving force ($\Delta pK_a = pK_a^{\text{cluster}} - pK_a^{\text{acid}}$) for all these protonation reactions are essentially the same. Consequently any difference in the rate constants for proton transfer is not attributable to a change in the driving force. (ii) All the rate constants for proton transfer

are significantly slower than the diffusion-controlled limit. It is important to bear in mind that the rate constants are for a proton transfer, which is thermodynamically unfavourable. We want to estimate the rate constant for proton transfer in a thermodynamically favourable reaction $\Delta pK_a = (pK_a^{\text{cluster}} - pK_a^{\text{acid}}) = +1.0$. The Brønsted equation [20] relates the rate constant for proton transfer to the equilibrium constant for thermodynamically unfavourable reactions ($k = G_A K^\alpha$) where G_A and α are constants for a series of similar acids, and $\alpha \leq 1$. When proton transfer is thermodynamically favourable the rate constant for the pro-

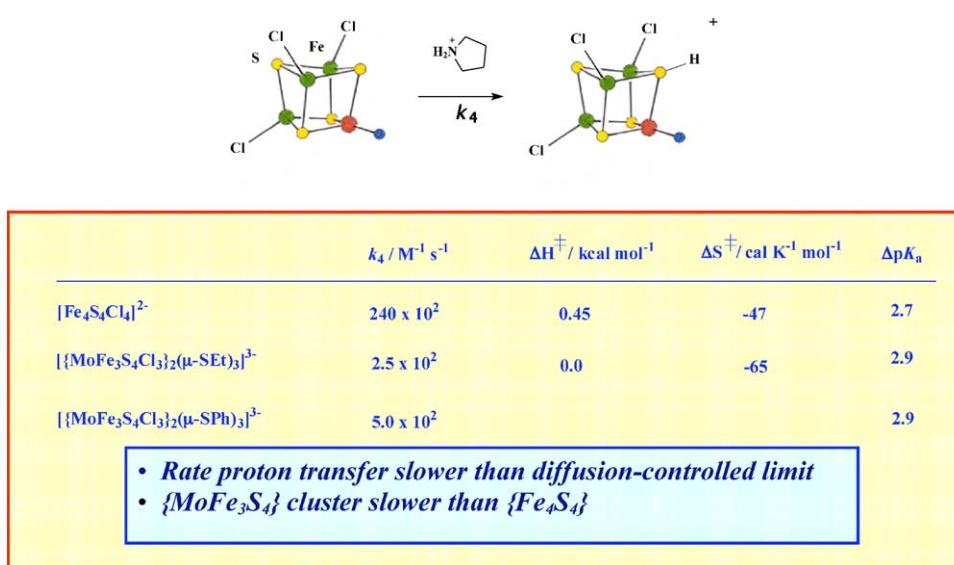


Fig. 13. Summary of the elementary rate constants for the reaction between Fe-S-based clusters and $[\text{H}_2\text{N}(\text{CH}_2)_3\text{CH}_2]^+$ in the presence of Br^- (weak nucleophile) in MeCN.

cess becomes independent of the driving force. Thus, for $[\text{Fe}_4\text{S}_4\text{Cl}_4]^{2-}$, knowing that $k_2 = 240 \times 10^2 \text{ dm}^3 \text{ mol}^{-1} \text{ s}^{-1}$ when $\Delta pK_a = (pK_a^{\text{cluster}} - pK_a^{\text{acid}}) = -2.8$ we can estimate that when $\Delta pK_a = (pK_a^{\text{cluster}} - pK_a^{\text{acid}}) = +1.0$, $k = \text{ca. } 4.8 \times 10^6 \text{ dm}^3 \text{ mol}^{-1} \text{ s}^{-1}$. Thus, the rate of protonation of $[\text{Fe}_4\text{S}_4\text{Cl}_4]^{2-}$ is ca. 10^4 times slower than the diffusion-controlled limit. This indicates that there is an intrinsic barrier to protonation of the cluster core. It has been suggested that the barrier is structural. Protonation of a $\mu_3\text{-S}$ must result in bond length changes to the three ligated Fe atoms. However, changes at these bonds will have effect on the other bonds within the cluster framework. Thus, all 12 bonds in the $\{\text{Fe}_4\text{S}_4\}$ cube (and also possibly the bonds to the four terminal Fe–Cl) have to adjust during the proton transfer leading to a slow reaction. We will discuss the evidence for structural changes in the next section. (iii) Finally, $[\{\text{MoFe}_3\text{S}_4\text{Cl}_3\}_2(\mu\text{-SEt})_3]^{3-}$ and $[\{\text{MoFe}_3\text{S}_4\text{Cl}_3\}_2(\mu\text{-SPh})_3]^{3-}$ protonate appreciably slower than $[\text{Fe}_4\text{S}_4\text{Cl}_4]^{2-}$. The reason for this is not entirely clear but it could be that the structural adjustments around the Mo in the cluster core are energetically more demanding than rearrangements about the Fe sites.

2.4. Electronic effects on the rates of proton transfer

The proposal that structural reorganisation of the cluster is a significant barrier to proton transfer in Fe–S-based clusters is supported by the results from studies on the rates of the reactions between $[\text{Fe}_4\text{S}_4\text{Cl}_4]^{2-}$ and $4\text{-RC}_6\text{H}_4\text{S}^-$ ($\text{R} = \text{MeO}$, Me , H , Cl or CF_3) [21] in the presence of $[\text{H}_2\text{N}(\text{CH}_2)_3\text{CH}_2]^+$. We have already described in the section above how studying the kinetics for the reaction between

$[\text{Fe}_4\text{S}_4\text{Cl}_4]^{2-}$ and $\text{C}_6\text{H}_5\text{S}^-$ both in the absence and presence of $[\text{H}_2\text{N}(\text{CH}_2)_3\text{CH}_2]^+$ allows us to calculate all the elementary rate constants shown in the mechanism in Fig. 10. A notable feature of the mechanism in Fig. 10, which we can make use of, is that proton transfer occurs after the attack of the nucleophile. Consequently, the rate of proton transfer will be subject to the electronic influence of the coordinated thiolate.

The effect that the 4-R-substituents on $4\text{-RC}_6\text{H}_4\text{S}^-$ have on k_1 , k_{-1} and k_2 are shown in the Hammett plot in Fig. 14. It is noteworthy and surprising that proton transfer to the cluster is subject to the same electronic effects as nucleophile binding. In particular, the addition of either a cation (H^+) or an anion (PhS^-) is facilitated by electron-withdrawing 4-R-substituents. It might have been anticipated that both k_1 and k_2 would be facilitated by electron-releasing groups which make the thiolate a better nucleophile (more electron-rich sulfur) and increase the basicity of the cluster site when the thiolate is coordinated.

The effect of the 4-R-substituent on k_1 seems most likely to be a transition state stabilisation effect. Upon approach of the anionic thiolate towards the anionic cluster there must be an unfavourable build-up of negative charge. Electron-withdrawing 4-R-substituents can dissipate the charge in the transition state. That electron-withdrawing 4-R-substituents on a thiolate ligand facilitate the transfer of a proton to the cluster indicates that in the transition state of the proton-transfer step there must also be an unfavourable build-up of negative charge.

In general, protonation of any site must involve shortening of the bond lengths of the ligands around that site. In the case

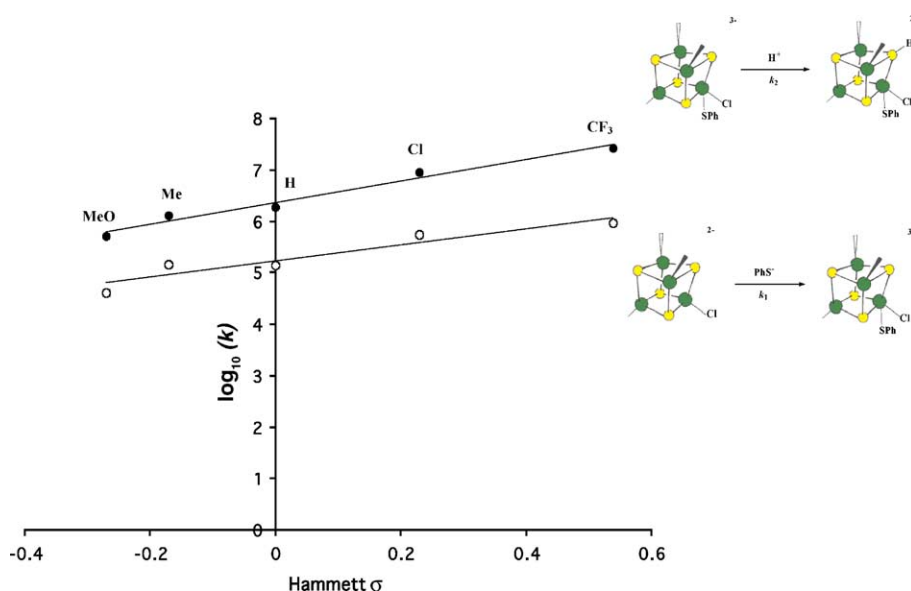


Fig. 14. Hammett plot for the elementary rate constants (k_1^R , k_{-1}^R and k_2^R) for the reaction between $[\text{Fe}_4\text{S}_4\text{Cl}_4]^{2-}$ and $[\text{H}_2\text{N}(\text{CH}_2)_3\text{CH}_2]^+$ in the presence of $4\text{-RC}_6\text{H}_4\text{S}^-$ ($\text{R} = \text{MeO}$, Me , H , Cl or CF_3) in MeCN.

of Fe–S-based clusters, the shortening of the Fe–thiolate bond will be resisted by the build-up of negative charge, as the thiolate and anionic cluster get closer. This negative charge can be dissipated by electron-withdrawing 4-R-substituents, thus facilitating the Fe–thiolate bond length changes and hence the rate of proton transfer. Thus, Fe–thiolate bond shortening prior to, or concomitant with, proton transfer could modulate the rate of proton transfer.

Earlier studies had indicated that electron-withdrawing R-substituents increase the rate of nucleophile binding, but in a manner which cannot be quantified [3,14].

3. Protonation and the action of nitrogenase

In the presentation so far, the ubiquitous nature of protonation of the cluster cores in synthetic Fe–S-based clusters has been emphasised. However, all of the work has been performed in MeCN. The question arises, “Does the analogous protonation chemistry of Fe–S-based clusters operate in a protic environment, with a pK_a for protonation of the cluster core in a range which is physiologically relevant?”

As outlined above, we have determined the pK_a 's of a variety of clusters, ranging from $[\text{Fe}_2\text{S}_2\text{Cl}_4]^{2-}$ to the so-called “basket clusters”. However, these pK_a 's are for a non-aqueous, aprotic environment. It is possible to estimate the pK_a in MeOH from the pK_a determined in MeCN using Eq. (1) [22] which gives $pK_a = 10.9 \pm 0.5$. However, this value is, at best, only approximate. Only with studies in a protic solvent can we determine the pK_a 's in a medium which is that associated with naturally occurring Fe–S clusters and hence judge whether the protonation reactions identified in MeCN for synthetic clusters are relevant to the action of proteins.

$$pK_a(\text{MeCN}) - 7.5 = pK_a(\text{MeOH}) \quad (1)$$

The kinetics of the reaction between the methanol soluble $[\text{Fe}_4\text{S}_4\{\text{SCH}_2\text{CH}(\text{OH})\text{Me}\}_4]^{2-}$ and PhS^- in the presence of $[\text{NHEt}_3]^+$ exhibits behaviour analogous to that described for the studies of $[\text{Fe}_4\text{S}_4(\text{SR})_4]^{2-}$ in MeCN. Using the kinetic data for the acid-catalysed substitution reaction we can calculate $pK_a = 8.5$ for $[\text{Fe}_4(\text{SH})\text{S}_3\{\text{SCH}_2\text{CH}(\text{OH})\text{Me}\}_4]^{2-}$ in MeOH. Thus, protonation of a $\mu_3\text{-S}$ in the $\{\text{Fe}_4\text{S}_4\}^{2+}$ core is associated with a pK_a which is physiologically significant.

Bruice et al. have also studied the substitution reactions of synthetic Fe–S clusters in aqueous solutions [23] and observed that the multiple substitution of $[\text{Fe}_4\text{S}_4(\text{SR})_4]^{2-}$ (R = alkyl) exhibited a pH dependence indicating a pK_a of the cluster of about 3.9. A similar pK_a was observed in the kinetics of dissolution of natural Fe–S clusters from high potential iron protein and five ferredoxins [24]. In another study, the cluster $[\text{Fe}_4\text{S}_4(\text{SCH}_2\text{CH}_2\text{CO}_2)_4]^{6-}$ was investigated [25]. In this last cluster, there is a high associated charge because the terminal thiolate ligands involve carboxylate residues. Spectrophotometric titration of this cluster with acid gave $pK_a = 7.4$. The higher pK_a of this cluster was attributed to the

electrostatic effect of the pendant carboxylate groups. It was proposed that the proton is associated with a Fe_2S_2 face with a hydrogen-bridged structure involving the filled d-orbitals above the face of the cluster. However, the evidence for such a novel structure is poor. The simple addition of the proton to the lone pair of electrons on the sulfur of the thiolate ligands or the $\mu_3\text{-S}$ atoms seems a much simpler and more reasonable proposal.

3.1. The binding of substrates by nitrogenases

The nitrogenases are a class of enzyme, which convert N_2 into NH_3 . There are three types of nitrogenase, which employ Fe–S-based clusters as the substrate binding and transformation site. The most common (and the most studied) type contains Mo and Fe, another contains V and Fe and the last contains only Fe. All three nitrogenases accomplish the transformation of N_2 under ambient conditions by a sequence of coupled electron- and proton-transfer reactions, with the substrate bound to a Fe–S-based cluster called cofactor. In the Mo-nitrogenase, the cofactor has the composition $\{\text{MoFe}_7\text{S}_9(\text{N})(R\text{-homocitrate})\}$, whilst in the V- and Fe-only-nitrogenases the Mo is replaced by V or Fe, respectively.

All three nitrogenases comprise two metalloproteins: the Fe-protein and the MFe-protein (M = Mo, V or Fe). Crystallographic data is only available for the Mo-nitrogenase so this is the form on which we will focus. In Mo-nitrogenase, the structure of active site has been established by X-ray crystallography (Fig. 15) [26–29].

The major role of the Fe-protein is the transfer of electrons from the external reductant (flavodoxin or ferredoxin) to the MFe-protein. The Fe-protein has been isolated and purified from a variety of different organisms. Irrespective of their origin, they are all much the same size ($M_r \sim 65$ kDa) and have an α_2 dimer structure with a single cuboidal $\{\text{Fe}_4\text{S}_4\}$ cluster bound between the subunits via cysteine amino acid residues [30].

The MoFe-protein isolated from a number of different bacterial sources are all similar with $M_r \sim 220$ kDa and an $\alpha_2\beta_2$ tetramer structure. The two $\alpha\beta$ dimers interact predominantly between the helices of the β -subunits at the tetramer interface [26–28]. A channel (diameter ca. 8 Å) goes through the centre of the tetramer. Each $\alpha\beta$ subunit contains two structurally unique Fe–S-based clusters: one P-cluster and one FeMo-cofactor.

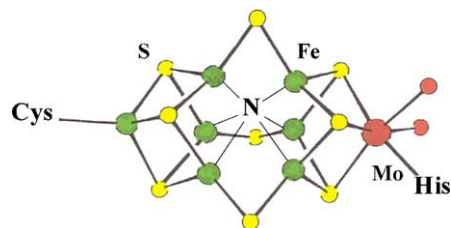


Fig. 15. Structure of FeMo-cofactor.

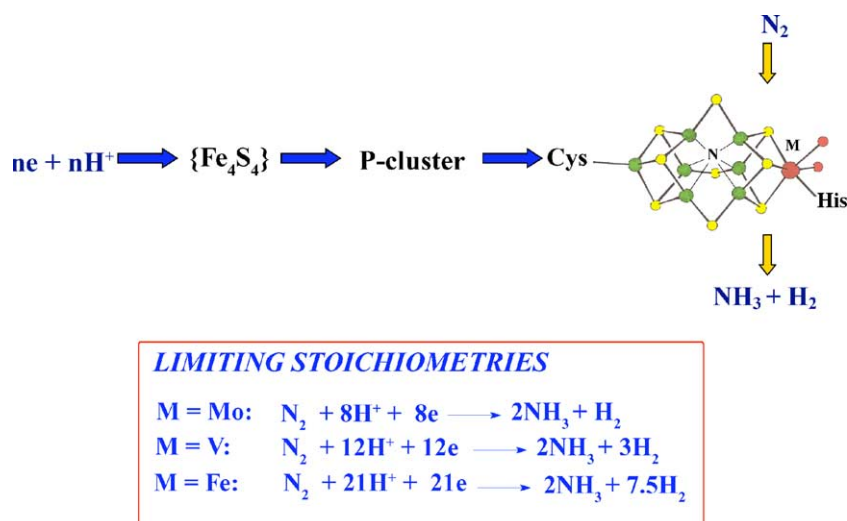


Fig. 16. Electron transfer sequence for nitrogenases, including the limiting stoichiometries of the Mo-, V- or Fe-only-nitrogenase.

The P-clusters almost certainly act as capacitors, storing electrons until they are required by the active site (FeMo-cofactor), for the conversion of N_2 into NH_3 . The FeMo-cofactor is enclosed within the α -subunit of the MoFe-protein, ca. 10 Å from the surface. The cofactor is bound to the polypeptide through Cys α 275 (to the terminal tetrahedral Fe) and His α 442 (to Mo). The Mo is six-coordinate with two of the sites occupied by *R*-homocitrate acting as a bidentate ligand, coordinated through alkoxy and carboxylate groups, with the carboxylate groups of the $-CH_2CH_2CO_2^-$ and $-CH_2CO_2^-$ arms being pendant.

At its crudest level, the mechanism of the nitrogenases is the electron transfer pathway shown in Fig. 16. In the absence of N_2 , all nitrogenases reduce H^+ to H_2 , and even in the presence of a large excess of N_2 the evolution of H_2 can never be completely suppressed. The production of H_2 by the nitrogenases is a natural consequence of the cofactor having to operate in a protic environment, where electrons are being fed to the active site. However, this production of H_2 wastes energy and leads to an inefficient enzyme. Not only is the enzyme producing a product (H_2), which is not wanted, but also the electrons supplied to the active site are being routed away from the desired product (NH_3). It is generally accepted that two molecules of ATP have to be hydrolysed for every electron transferred. If the electrons are not being employed in the transformation of N_2 then the production of each molecule of H_2 involves the waste of the energy supplied by hydrolysis of four molecules of ATP.

The three nitrogenases have very different efficiencies as shown by the limiting stoichiometries in Fig. 16. Thus, the Mo-based nitrogenase is the most efficient, producing only one H_2 for every two molecules of NH_3 formed; whilst the Fe-only nitrogenase is the least efficient producing about 7.5 H_2 for every two molecules of NH_3 formed, and the V-based nitrogenase lies in the middle, producing three H_2 for every two molecules of NH_3 . Since the only difference between the

cofactors in the three nitrogenases is the presence of the Mo, V or Fe it appears that the metal composition of the cluster core is influencing the relative abilities of the cofactor to fix N_2 on the one hand, or reduce H^+ to H_2 on the other.

3.2. Protonation of nitrogenase cofactors and dihydrogen production

A natural consequence of the chemistry that the cofactors perform (transformation of N_2 and other substrates by sequences of electron- and proton-transfer reactions) means these Fe–S-based clusters must operate in a protic environment. Both theoretical [31] and experimental studies [12] on extracted FeMo-cofactor from the Mo-based nitrogenase indicate protonation of μ_2 -S or μ_3 -S sites. Clearly, this is line with the prevalent protonation chemistry observed with synthetic Fe–S-based clusters: the cofactors of nitrogenase are doing nothing more than what is natural for Fe–S cluster. The important point is that this protonation of the cluster core in the presence of a supply of electrons can lead to the reduction of H^+ to H_2 , which in its turn leads to inefficiency in the nitrogen fixing ability of the enzyme since electrons that could be used for converting N_2 into NH_3 are being wasted in the production of H_2 .

In the presence of N_2 , the evolution of H_2 is suppressed and some NH_3 is produced. However, H_2 production cannot be entirely suppressed. At high pressures of N_2 , a limiting stoichiometry is reached as described in Fig. 16. Under these conditions, some H_2 is still evolved and, for the Mo nitrogenase, about one molecule of H_2 is produced for every molecule of N_2 converted into NH_3 . This limiting stoichiometry led to the proposal that N_2 bound to the active site by displacing H_2 from a metal-hydride site [32]. The discovery of other types of nitrogenases with very different limiting stoichiometries has led to a reconsideration of this proposal.

Two other nitrogenases have been established [30]: the V-nitrogenase contains V and Fe and the Fe-only-nitrogenase contains just Fe. The V-nitrogenase contains a cofactor in which V has formally replaced Mo whilst in the Fe-only nitrogenase the Mo has formally been replaced by Fe. This difference between the various nitrogenases amounts only to a single metal in the cofactor. Yet this appears to have a profound effect on the product specificities of the nitrogenases. Most notably, the three nitrogenases have very different limiting stoichiometries.

Our work on the protonation chemistry, and notably the rates of proton transfer, of synthetic Fe–S-based clusters allow us to now rationalise these relative efficiencies of the nitrogenases and how change of a single metal in the cluster can lead to significant changes in efficiency. Fig. 17 shows an outline representation of the key steps in the initial stages of nitrogen fixation. On the right hand side is the binding of dinitrogen to the reduced cofactor, and on the left hand side is the protonation of the cofactor and the subsequent reduction of protons to dihydrogen. For an efficient nitrogen fixing system, the cluster needs to maximise the possibility for the reactions on the right and minimise the reactions on the left. This is a major logistic problem for any nitrogen fixing system since (in order to convert dinitrogen into ammonia) it is an essential requirement that protons are present around the active site.

Our work on synthetic Fe–S-based clusters indicates that, irrespective of where dinitrogen binds on cofactor, Mo affects the reactivity of the cofactor in a way which facilitates efficient nitrogen fixation by making protonation of the cluster slow which in its turn suppresses dihydrogen production. Proton transfer to all Fe–S cluster cores is slow (at least 10^4 times slower than the diffusion-controlled limit) and, most important, Mo–Fe–S clusters protonate appreciably slower than Fe–S-only clusters. That Mo in synthetic Fe–S-based clusters makes proton transfer to the clusters slow is advantageous for a site whose role is to fix dinitrogen.

Mo may also facilitate nitrogen fixation by “assisting” the binding of the substrate. Studies on $[\text{Fe}_4\text{S}_4(\text{SEt})_4]^{2-}$ and $[\{\text{MoFe}_3\text{S}_4(\text{SEt})_3\}_2(\mu-\text{SEt})_3]^{3-}$ show that the Mo-containing cluster has a higher binding affinity for a range of small molecules and ions (e.g., halide, N_3^- , CN^- , N_2O). In these clusters, the Mo is six-coordinate and thus it seems likely that the molecules and ions are binding to the Fe sites [6]. Thus, the presence of Mo in the cluster core is making the Fe sites behave as though they are more electron-deficient than in $[\text{Fe}_4\text{S}_4(\text{SEt})_4]^{2-}$.

The presence of Mo in FeMo-cofactor may facilitate nitrogen fixation in the following ways: (i) by slowing protonation of the active site and hence wasteful dihydrogen production; (ii) by increasing the affinity of the Fe sites to bind substrates relative to Fe–S-only clusters. Thus, the presence of Mo in cofactor could facilitate nitrogen fixation not only by favouring binding of the substrate but also ensuring that the enzyme is a good nitrogenase but a poor hydrogenase.

4. Summary

This article has focussed on the protonation chemistry of synthetic Fe–S-based cluster and shown how some general reactivity patterns have emerged from studies on the synthetic clusters, which might reasonably be expected to operate in natural Fe–S-based clusters. Protonation of synthetic Fe–S-based clusters is common place but cannot be detected directly because of the poor spectroscopic response. The development of a kinetic method whereby protonation is effectively coupled to substitution has resulted in an understanding of how many protons bind to clusters, indications of where they bind and how protonation affects the substitution lability of the terminal ligands on the cluster. In addition, studies on the rates of proton transfer to synthetic Fe–S-based clusters have indicated that even for thermodynamically favourable reactions protonation of $[\text{Fe}_4\text{S}_4\text{Cl}_4]^{2-}$

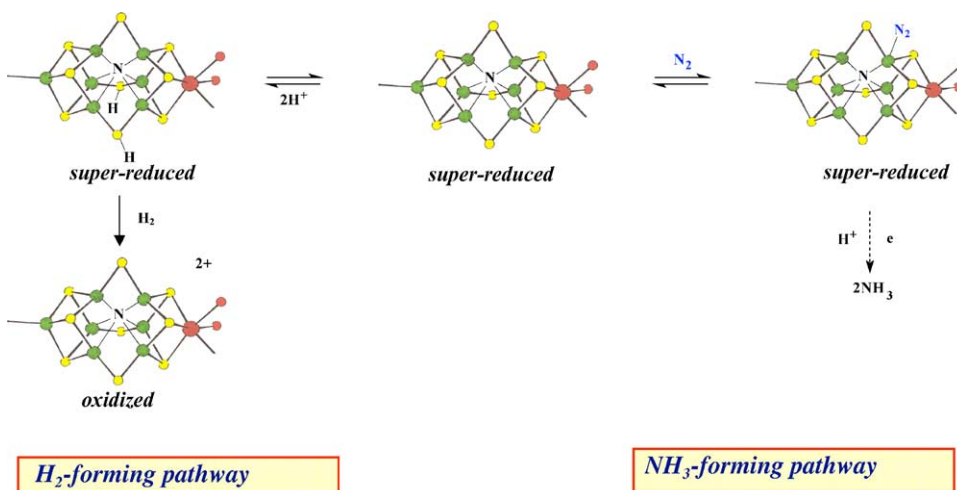


Fig. 17. Outline of the competitive pathways in which the FeMo-cofactor binds and transforms N₂ (right hand side), or binds protons and produces H₂.

occurs about 10^4 times slower than the diffusion-controlled limit.

The biological role of FeMo-cofactor (a natural Fe–S-based cluster) in nitrogenase is to convert N_2 into NH_3 by a sequence of coupled electron- and proton-transfer reactions. It is evident that the cofactor must operate in a protic environment. Protons have deleterious effect on the action of the cofactor since, in the absence of substrate, nitrogenase reduces protons to H_2 , and this reaction cannot be entirely suppressed even in the presence of large amounts of the substrate. The work on synthetic Fe–S-based clusters offers a possible model for how the cofactor operates in a protic environment and such studies are beginning to piece together how the constituent metals of FeMo-cofactor contribute to the overall reactivity of the cluster.

References

- [1] (a) R.H. Holm, P. Kennepohl, E.I. Solomon, *Chem. Rev.* 96 (1996) 2239;
(b) H. Matsubara, K. Saeki, *Adv. Inorg. Chem.* 38 (1992) 223;
(c) R. Cammack, *Adv. Inorg. Chem.* 38 (1992) 281.
- [2] (a) P.A. Lindahl, *Biochemistry* 41 (2002) 2097;
(b) T.I. Doukov, T.M. Iverson, J. Seravalli, S.W. Ragsdale, C.L. Drennan, *Science* 298 (2002) 567;
(c) C. Darnault, A. Volbeda, E.J. Kim, P. Legarand, X. Vernede, P.A. Lindahl, J.C. Fontecilla-Camps, *Nat. Struct. Biol.* 100 (2003) 3689;
(d) J.B. Howard, D.C. Rees, *Chem. Rev.* 96 (1996) 2965;
(e) B.K. Burgess, D.J. Lowe, *Chem. Rev.* 96 (1996) 2983;
(f) G. Leigh (Ed.), *Nitrogen Fixation at the Millenium*, Elsevier, Amsterdam, 2002;
(g) J.C. Fontecilla-Camps, *J. Biol. Inorg. Chem.* 1 (1996) 91;
(h) M. Frey, *Structure* 90 (1998) 98;
(i) J.W. Peters, W.N. Lanzilotta, B.J. Lemon, L.C. Seefeldt, *Science* 282 (1998) 1853.
- [3] G.R. Dukes, R.H. Holm, *J. Am. Chem. Soc.* 97 (1975) 528.
- [4] R.A. Henderson, K.E. Oglieve, *J. Chem. Soc., Dalton Trans.* (1993) 1467.
- [5] R.A. Henderson, K.E. Oglieve, *J. Chem. Soc., Chem. Commun.* (1994) 1961.
- [6] R.A. Henderson, K.E. Oglieve, *J. Chem. Soc., Dalton Trans.* (1993) 1473.
- [7] J.F. Coetzee, *Prog. Phys. Org. Chem.* 4 (1967) 45.
- [8] G. Cauquis, A. Deronzier, D. Serve, E. Vieil, *J. Electroanal. Chem. Interfacial Electrochem.* 60 (1975) 205.
- [9] K. Izutsu, *Acid–Base Dissociation Constants in Dipolar Aprotic Solvents*, Blackwell Scientific, Oxford, 1990.
- [10] R.A. Henderson, K.E. Oglieve, *J. Chem. Soc., Dalton Trans.* (1999) 3927.
- [11] R.A. Henderson, K.E. Oglieve, *J. Chem. Soc., Chem. Commun.* (1994) 377.
- [12] V.R. Almeida, C.A. Gormal, K.L.C. Gronberg, R.A. Henderson, K.E. Oglieve, B.E. Smith, *Inorg. Chim. Acta* 291 (1999) 212.
- [13] A.J. Dunford, R.A. Henderson, *Chem. Commun.* (2002) 360.
- [14] K.L.C. Gronberg, R.A. Henderson, *J. Chem. Soc., Dalton Trans.* (1996) 3667.
- [15] K.L.C. Gronberg, R.A. Henderson, K.E. Oglieve, *J. Chem. Soc., Dalton Trans.* (1997) 1507.
- [16] Z. Cui, R.A. Henderson, *Inorg. Chem.* 41 (2002) 4158.
- [17] D. Sellmann, J. Sutter, *Acc. Chem. Res.* 30 (1997) 460.
- [18] R.A. Henderson, K.E. Oglieve, *J. Chem. Soc., Dalton Trans.* (1998) 1731.
- [19] J. Bell, A.J. Dunford, E. Hollis, R.A. Henderson, *Angew. Chem. Int. Ed.* 42 (2003) 1149.
- [20] R.P. Bell, *The Proton in Chemistry*, second ed., Chapman and Hall, London, 1973, p. 195.
- [21] A.J. Dunford, R.A. Henderson, *Chem. Commun.* (2002) 360.
- [22] E.P. Capellani, S.D. Drouin, G. Jia, P.A. Maltby, R.H. Morris, C.T. Schweitzer, *J. Am. Chem. Soc.* 116 (1994) 3375 (Ref. [21]).
- [23] T.C. Bruice, R. Maskiewicz, R. Job, *Proc. Nat. Acad. Sci. U.S.A.* 72 (1975) 231.
- [24] R. Maskiewicz, T.C. Bruice, *Biochemistry* 16 (1977) 3024.
- [25] R.C. Job, T.C. Bruice, *Proc. Nat. Acad. Sci. U.S.A.* 72 (1975) 2478.
- [26] J. Kim, D.C. Rees, *Science* 257 (1992) 1677.
- [27] J. Kim, D.C. Rees, *Nature* 360 (1992) 553.
- [28] J.W. Peters, M.H.B. Stowell, S.M. Soltis, M.C. Finnegan, M.K. Johnson, D.C. Rees, *Biochemistry* 36 (1997) 118.
- [29] O. Einsle, F.A. Teczan, S.L.A. Andrade, B. Schmid, M. Yoshida, D.C. Rees, *Science* 297 (2002) 1696.
- [30] R.R. Eady, *Chem. Rev.* 96 (1996) 3013.
- [31] I.G. Dance, *Chem. Commun.* (1998) 523.
- [32] R.N.F. Thorneley, D.J. Lowe, in: T. Spiro (Ed.), *Molybdenum Enzymes*, Wiley–Interscience, New York, 1985, p. 221.